Bi-Solitons on the Surface of a Deep Fluid: An Inverse Scattering Transform Perspective Based on Perturbation Theory

Andrey Gelash,[1,*] Sergey Dremov,[3] Rustam Mullyadzhanov,[2,4] and Dmitry Kachulin[2,3]
[1]*Laboratoire Interdisciplinaire Carnot de Bourgogne (ICB), UMR 6303 CNRS—Université Bourgogne Franche-Comté, 21078 Dijon, France*
[2]*Novosibirsk State University, Novosibirsk 630090, Russia*
[3]*Skolkovo Institute of Science and Technology, Moscow 121205, Russia*
[4]*Institute of Thermophysics SB RAS, Novosibirsk 630090, Russia*

(Received 7 November 2023; accepted 13 February 2024; published 28 March 2024)

We investigate theoretically and numerically the dynamics of long-living oscillating coherent structures —bi-solitons—in the exact and approximate models for waves on the free surface of deep water. We generate numerically the bi-solitons of the approximate Dyachenko-Zakharov equation and fully nonlinear equations propagating without significant loss of energy for hundreds of the structure oscillation periods, which is hundreds of thousands of characteristic periods of the surface waves. To elucidate the long-living bi-soliton complex nature we apply an analytical-numerical approach based on the perturbation theory and the inverse scattering transform (IST) for the one-dimensional focusing nonlinear Schrödinger equation model. We observe a periodic energy and momentum exchange between solitons and continuous spectrum radiation resulting in repetitive oscillations of the coherent structure. We find that soliton eigenvalues oscillate on stable trajectories experiencing a slight drift on a scale of hundreds of the structure oscillation periods so that the eigenvalue dynamics is in good agreement with predictions of the IST perturbation theory. Based on the obtained results, we conclude that the IST perturbation theory justifies the existence of the long-living bi-solitons on the surface of deep water that emerge as a result of a balance between their dominant solitonic part and a portion of continuous spectrum radiation.

DOI: 10.1103/PhysRevLett.132.133403

Formation of stable localized coherent structures—solitons—is one of the key evolution scenarios of nonlinear wave systems [1]. When such a system is Hamiltonian, solitons emerge due to a balance between nonlinearity and dispersion, while in nonconservative cases, an additional balance between energy gain and loss comes into play [1–3]. Being described by nonlinear partial differential equations (PDEs), systems with solitons can be seen in almost all fields of physics—for example, in hydrodynamics, optics, and plasmas [2,4]. While individual stationary solitons are ubiquitous for nonlinear wave models, long-living multisoliton complexes are not so common and thus draw particular attention and are of great interest for experimental implementation. For example, a bound state of solitons has been observed in mode-locked fiber lasers, Bose-Einstein condensates, and specially designed optical waveguides [5–8].

For a Hamiltonian wave model the presence of recursive multisoliton behavior might be a signature of its integrability or nearly integrable dynamics [9–12]. The inverse scattering transform (IST) theory elucidates the particlelike features of solitons in exactly integrable nonlinear PDEs by proving that solitons correspond to the time-invariant eigenvalue spectrum of an auxiliary scattering problem [9,13]. For example, solitons of the integrable one-dimensional nonlinear Schrödinger equation (NLSE) collide elastically, forming bouncing multisoliton complexes, and preserve their parameters during the whole system evolution [14]. When integrability is broken by adding weak extra terms to the model, solitons can still form long-living but usually inelastic complexes radiating incoherent waves, whose dynamics is described by the IST perturbation theory [10,15,16].

We consider the Hamiltonian models of the 2D hydrodynamics with a free surface: (i) focusing NLSE [17], (ii) Dyachenko-Zakharov envelope equation (DZE) [18], and (iii) fully nonlinear equations for the R-V variables (RVE) [19–22]. These models are the members of the Hamiltonian hierarchy of equations for the free surface water waves [17,23] in which the NLSE describes only the weakly nonlinear narrow-banded wave trains while the DZE captures many of the nonlinear effects presented in the full model [17,18]. Comparative analysis of the behavior of wave groups in the approximate DZE and the exact RVE models provides insights into how the model objects are expected to be seen in nature [24–26].

Numerical works revealed solitary waves for the DZE and RVE models [27,28] observed later in water wave tank experiments [29,30]. For certain parameters, pairwise collisions of the DZE solitons do not produce any visible

radiation [31], which can be detected only in multiple collisions [32] demonstrating nearly integrable regimes of the DZE model. In addition, recent numerical studies discovered extremely long-living bi-solitons in both DZE and RVE [33,34]. The theoretical description of such recursive coherent complexes on the surface of a deep fluid, their internal structure, and their interaction mechanisms remains an open questions. To understand it, we propose an analytical-numerical approach based on the IST theory for our theoretical benchmark model: the NLSE. The IST analysis unveils stable trajectories of soliton eigenvalues and shows that the long-living bi-solitons on the surface of deep water emerge as a result of a balance between their dominant solitonic part and a portion of incoherent radiation. Finally the IST perturbation theory demonstrates that both the DZE and RVE bi-soliton oscillatory complexes exist in nearly integrable regimes of the NLSE.

The original equations describing 2D hydrodynamics of deep water waves propagating on the free surface of an ideal incompressible fluid in the presence of gravity represent the Laplace equation with kinematic and dynamic boundary conditions at the surface:

$$\begin{aligned} &\phi_{xx}+\phi_{yy}=0 \quad \text{with} \quad \phi_y\to 0 \quad \text{at } y\to-\infty,\\ &\eta_t+\eta_x\phi_x=\phi_y \quad \text{at } y=\eta,\\ &\phi_t+(\phi_x^2+\phi_y^2)/2+g\eta=0 \quad \text{at } y=\eta. \end{aligned} \tag{1}$$

Here, x and y are horizontal and vertical coordinates, t is time, g is the free-fall acceleration, $\eta(x,t)$ is the shape of the surface, $\phi(x,y,t)$ is a hydrodynamic potential inside the fluid. Classical problem (1) has been known since the 19th century [35] and now represent a backbone of theoretical, numerical, and experimental studies [36–39].

The Hamiltonian of system (1) is [17]

$$H=\frac{1}{2}\int dx\int_{-\infty}^{\eta}|\nabla\phi|^2dy+\frac{g}{2}\int\eta^2dx. \tag{2}$$

For the numerical solution of the fully nonlinear equations we apply conformal mapping of the fluid domain $z=x+iy$ confined by a free boundary onto the lower half-plane of the new complex variable $w=u+iv$ at $v\le 0$. In terms of special analytical functions $R(u,t)$ and $V(u,t)$, original equations (1) turn into the RVE

$$\begin{aligned} R_t&=i(UR_w-RU_w),\\ V_t&=i(UV_w-RB_w)+g(R-1), \end{aligned} \tag{3}$$

with the following boundary conditions: $R\to 1$, $V\to 0$ at $v\to-\infty$; see [19,20,22] for the conformal mapping technique and Eq. (3) derivation. We define here $U=\hat{P}(VR^*+V^*R)$ and $B=\hat{P}(VV^*)$, where $\hat{P}=(1+i\hat{H})/2$, and $\hat{H}$ is the Hilbert transform.

Assuming the wave steepness to be small, $\mu=\eta_x\ll 1$, one can expand Hamiltonian (2) up to the fourth order of $\eta(x,t)$ and $\phi(x,\eta,t)$ and find the DZE for an approximate description of the water wave train in terms of canonical complex envelope variable $C(x,t)$ [18]:

$$\begin{aligned} iC_t=\hat{\theta}_{k_0+k}\Big[&(\hat{\omega}_{k_0+k}-\hat{\omega}_{k_0})C+i\frac{\partial\omega_k}{\partial k}\Big|_{k_0}C_x\\ &+k_0^2(|C|^2C)+i\big(\hat{k}(|C|^2)C+i|C|^2C_x\big)_x\\ &-ik_0\big(C(|C|^2)_x+2|C|^2C_x-i\hat{k}(|C|^2)C\big)\Big]. \end{aligned} \tag{4}$$

Operators $\hat{k}$ and $\hat{\omega}_k$ are multiplied by $|k|$ and $\sqrt{g|k|}$ in Fourier space, respectively, $\hat{\theta}_k$ is the Heaviside step function, k_0 is a characteristic carrier wave number, and $\omega_{k_0}=\sqrt{gk_0}$ is the corresponding linear frequency related to characteristic period of the waves $\tau_0=2\pi/\omega_{k_0}$. Models (3) and (4) being advantageous for analytical and numerical treatment are used in fundamental studies and find applications in deterministic wave forecasting [40–43].

Under the additional assumption of narrow-band wave spectrum, we obtain the remaining model of our hierarchy: the NLSE written in terms of complex envelope variable $q(x,t)$,

$$iq_t+q_{xx}/2+|q|^2q=0. \tag{5}$$

Being integrable, the NLSE exhibits exact multisoliton solutions, $q_N^S(x,t)$, where N is the number of solitons. The simplest single soliton solution represents the well-known expression

$$q_1^S(x,t)=a_1\frac{\exp[iv_1(x-x_1)+i(a_1^2-v_1^2)t/2+i\theta_1]}{\cosh a_1(x-v_1t-x_1)}, \tag{6}$$

with real-valued parameters a_1, v_1 for soliton amplitude and velocity and θ_1 and x_1 for its phase and position.

We generate long-living bi-solitons of the DZE and RVE numerically, which oscillate without significant loss of energy for hundreds of the structure periods T, which is $\sim 10^5\tau_0$ in dimensional units, similar to that in [27,28,34]. We set initial conditions using the two-soliton solution $q_2^S(x)$ of the NLSE characterized by different soliton amplitudes and zero velocities. Then, we substitute such standing bi-soliton complex into the considered equations. Not being a solution to the DZE or RVE, the initial structure emits incoherent waves at the beginning of the evolution. We absorb these waves by damping at the edges of the computational domain, allowing the structure to gradually find its stable, long-living state. Later, we turn off the damping and observe that the remaining structure propagates stably for hundreds of characteristic structure periods without losing energy. We present an example of

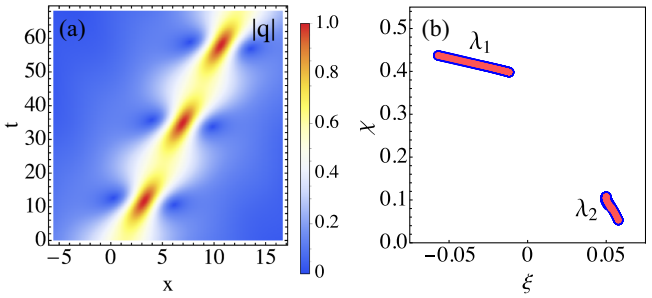

FIG. 1. Nonlinear behavior of the DZE bi-soliton. (a) Spatiotemporal diagram of the wave field envelope $|q_{(\mathrm{DZE})}|$ with characteristic oscillation period $T \approx 24.5$. (b) Stable trajectories of soliton eigenvalues obtained as a union of the computed time series of $\lambda(t_j)$. Blue and red lines correspond to two complete cycles of the bi-soliton oscillations separated by 200 T.

spatiotemporal oscillating dynamics of the DZE bi-soliton in Fig. 1(a) in terms of dimensionless wave field envelope. In addition, Fig. 4 shows the free surface profiles in dimensional units of bi-soliton in the RVE at minimum and maximum amplitude. More examples of the bi-soliton dynamics including animation of the wave field evolution and details on the numerical procedure used are given in Supplemental Material [44].

Our approach to analyzing bi-solitons starts with writing the NLSE for the complex-valued wave field envelope $q(x,t)$ with the right-hand side (rhs) in a general form

$$\begin{aligned} &\mathrm{NLSE}[q(x,t)] = \mathrm{rhs}[q(x,t)], \\ &\mathrm{NLSE}[q(x,t)] \equiv iq_t + q_{xx}/2 + |q|^2 q. \end{aligned} \tag{7}$$

We obtain the DZE and RVE wave fields in terms of $q(x,t)$ by applying the corresponding transformations between models (3), (4) and the NLSE:

$$q_{(\mathrm{DZE})} = q\{C(x,t)\}, \qquad q_{(\mathrm{RVE})} = q\{R(u,t), V(u,t)\}. \tag{8}$$

See Supplemental Material [44] for details. We can directly substitute $q_{(\mathrm{DZE/RVE})}$ into the NLSE and calculate not zero, but residual, which is exactly the rhs for (7):

$$\mathrm{rhs}_{(\mathrm{DZE/RVE})} = \mathrm{NLSE}[q_{(\mathrm{DZE/RVE})}]. \tag{9}$$

When $\mathrm{rhs} \equiv 0$, system (7) is integrable and associated with the following linear auxiliary Zakharov-Shabat system for a vector wave function $\Phi = (\phi_1, \phi_2)^{\mathrm{T}}$:

$$\hat{\mathcal{L}}\Phi = \lambda\Phi, \qquad \hat{\mathcal{L}} = \begin{pmatrix} i\partial_x & -iq(x) \\ -iq^*(x) & -i\partial_x \end{pmatrix}, \tag{10}$$

where $\lambda = \xi + i\chi$ is the time-independent complex spectral parameter and T means transposition. Solving the scattering problem for (10) at certain time, one finds the wave field IST spectrum (scattering data) consisting of a set of discrete eigenvalues and norming constants $\{\lambda_n, \rho_n\}$, $n = 1, \ldots, N$ with $\chi_n > 0$ and the reflection coefficient $r(\xi)$. The first discrete part of the IST spectrum corresponds to N solitons having parameters connected to the set $\{\lambda_n, \rho_n\}$ as

$$\begin{aligned} &\xi_n = v_n/2, \qquad \chi_n = a_n/2, \\ &\rho_n = 2i\chi_n \exp[i\pi - 2i\lambda_n x_n - i\theta_n]. \end{aligned} \tag{11}$$

Meanwhile, the reflection coefficient $r(\xi)$ being associated with the continuous part of $\hat{L}$ spectrum describes nonlinear dispersive radiation.

The IST theory proves that $\{\lambda_n\}$ and $|r(\xi)|$ do not change when $q(x)$ evolves according to the NLSE and only soliton phases and positions and the phases of the radiation run trivially in time [9,11]. As such, the IST spectrum represents a nonlinear analog of conventional Fourier harmonics that is broadly used in nonlinear wave field analysis [26,38,46–52]. When $r(\xi) = 0$ the wave field is composed of solitons only and its evolution can be described with the exact N-soliton solution $q_N^S(x,t)$; see [9,53] and Supplemental Material [44] for background on the IST formalism and exact multisoliton formulas.

In a general case when $\mathrm{rhs} \neq 0$, system (7) is no longer integrable and the IST eigenvalues are not stationary. However, when the NLSE part in (7) dominates on the rhs, one can apply the perturbation theory and express the evolution of the eigenvalues as [54,55] follows:

$$\frac{\partial\lambda}{\partial t} = \frac{\langle\Phi^\dagger, \widehat{\mathrm{rhs}}\Phi\rangle}{\langle\Phi^\dagger, \Phi\rangle}, \qquad \widehat{\mathrm{rhs}} = \begin{pmatrix} 0 & -\mathrm{rhs} \\ \mathrm{rhs}^* & 0 \end{pmatrix}, \tag{12}$$

where $\Phi^\dagger = (\phi_2^*, \phi_1^*)^{\mathrm{T}}$ and the scalar product $\langle f, g\rangle = \int_{-\infty}^{\infty} f^* g dx$. Formulation (7) together with equations (10) and (12) are the basis of the classical IST perturbation theory for which many exactly solvable cases of certain rhs's have been studied previously; see [10,56] and also some recent works [57,58]. However, many physically important, nearly integrable systems are left without consideration because their rhs is too complicated.

In our approach we do not require the rhs term in an explicit form and instead deal with discrete wave fields $q_{(\mathrm{DZE/RVE})}(x_i, t_j)$ obtained from simulations and use a combination of analytical and numerical IST tools to analyze them. We begin with bi-solitons in the DZE and, at first, solve the scattering problem for a series of time-evolving wave field profiles numerically using the algorithms [59–61]; see details in Supplemental Material [44]. We find two discrete eigenvalues $\lambda_1(t_j)$ and $\lambda_2(t_j)$ and nonzero reflection coefficient $r(\xi, t_j)$ as functions of t_j. The eigenvalues corresponding to solitons of the bi-soliton structure oscillate on stable trajectories during hundreds of T; see Fig. 1(b). Note, that solitons have nonzero velocities describing by the real part of λ. With the computed full set of scattering data, we represent the wave field at each

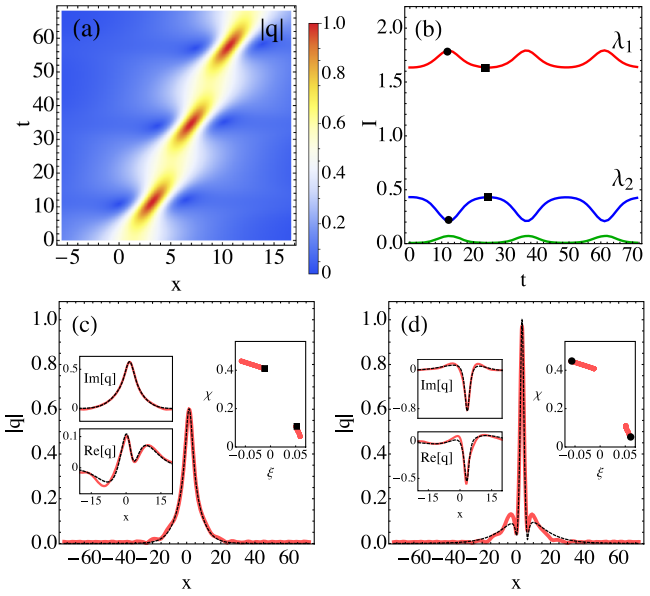

FIG. 2. Further IST analysis of the DZE bi-soliton. (a) Spatio-temporal dynamics of the two-soliton model (13). (b) Time evolution of I for each component of the IST spectrum: red and blue lines correspond to λ_1 and λ_2, respectively, while the green line shows the impact of continuous spectrum radiation. Panels (c) and (d) show the DZE wave field (red solid lines) at minimum (c) and maximum (d) amplitude, together with the model (13) (black dashed lines). Insets in (c) and (d) show real and imaginary parts of the wave fields and also indicate the eigenvalue locations by black squares and dots.

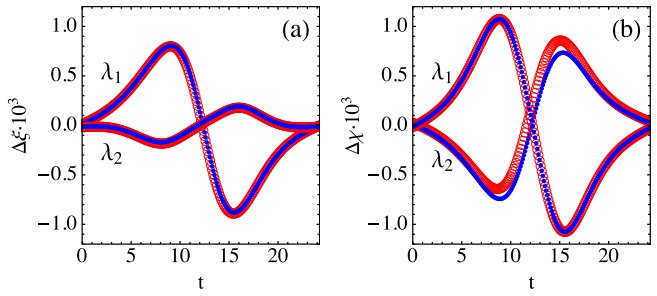

FIG. 3. Changes of discrete eigenvalues $\Delta\lambda_j = \Delta\xi_j + i\Delta\chi_j$ at each time step t_j within one oscillation period T of the DZE bi-soliton. Panels (a) and (b) correspond to $\Delta\xi$ and $\Delta\chi$ respectively. Blue dots show the direct numerical computation of soliton eigenvalues changes for each subsequent wavefield $q(t_j)$ and $q(t_{j+1})$. Red circles correspond to predictions of the perturbation theory provided by Eq. (12).

moment of time as two NLSE solitons and continuous spectrum radiation. To measure the impact of each scattering data component in the wave field composition, we use the NLSE integral of motion $I = \int_{-\infty}^{\infty} |q|^2 dx$, which can be evaluated individually for discrete spectrum eigenvalues as I^{DS} and continuous spectrum I^{CS} within the IST [9], so that $I = I^{\mathrm{DS}} + I^{\mathrm{CS}}$; see details in Supplemental Material [44].

At the edge trajectory points, the bi-soliton exhibits minimum or maximum of its intensity; see Fig. 2. We find that at the minimum intensity configuration, the impact of the continuous spectrum $I^{\mathrm{CS}}/I \approx 0.005$ is negligible, and the wave field represents almost the exact NLSE bi-soliton; see Fig. 2(a). During the structure evolution, the role of the radiation increases, reaching its maximum $I^{\mathrm{CS}}/I \approx 0.036$ at the other edge point; see Fig. 2(b). In other words an NLSE bi-soliton taken at the minimum intensity configuration evolves as a long-living oscillating complex stabilized by a minor radiation gradually increasing up to the high-amplitude wave field configuration. In contrast, an arbitrary choice of soliton eigenvalues leads to a formation of unstable trajectories that we illustrate in Supplemental Material [44]. The two solitons and radiation are in periodic energy exchange, which we demonstrate in Fig. 2(b) using time dependence of I for each part of the scattering data. We measure the radiation only in the space region of the bi-soliton having width $\sim$70.0; meanwhile, the impact of the rest part of the computational domain, where some small wave field oscillations can also be seen, contributes $\sim 10^{-3} I$, and thus can be neglected. The latter means that the bi-soliton exists on its own and does not participate in resonances with continuous waves typical for some nonlinear wave systems [62–64].

We find that the major dynamics of the DZE bi-solitons can be described by the exact two-soliton solution of the NLSE with dynamically changing eigenvalues and norming constants as

$$q_{(\mathrm{DZE})}(x, t_j) = q_2^{\mathrm{S}}(x, t_j; \{\lambda_n(t_j), \rho_n(t_j)\}). \tag{13}$$

Here, $\{\lambda_n(t_j), \rho_n(t_j)\}$, $n = 1, 2$ are the set of the computed time series of the discrete IST spectrum. Figure 2 illustrates the model (13) and its comparison with the initial bi-soliton wave fields. Then we compute the soliton eigenvalue changes at each time step as $\Delta\lambda(t_j) = \lambda(t_{j+1}) - \lambda(t_{j-1})$, and compare them with predictions of the perturbation theory. We find that Eq. (12) provides an excellent description for both solitons; see Fig. 3. To evaluate the integral in Eq. (12) we use numerically computed $\mathrm{rhs}_{(\mathrm{DZE})}(x_i, t_j)$ and wave functions $\Phi(x_i, t_j)$; see details in Supplemental Material [44]. Our analysis shows that the DZE bi-soliton complex exists in a nearly integrable regime.

Finally, we study the long-living RVE bi-soliton and obtain qualitatively similar results as for the DZE case. Figure 4(a) shows the surface elevation in physical units corresponding to the minimum and maximum of the RVE bi-soliton intensity. Applying transformation (8) we obtain the bi-soliton envelope $q_{(\mathrm{RVE})}(x, t_j)$ oscillating with $T \approx 30.0$ and compute the soliton eigenvalue trajectories; see Fig. 4(b). The trajectories are slightly perturbed in comparison to the DZE case and experience a minor drift on a scale of hundreds of bi-soliton oscillation periods. The rest of the IST analysis repeats our results for the DZE and is

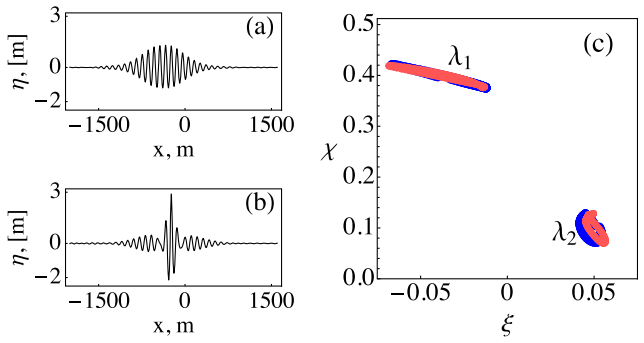

FIG. 4. Nonlinear behavior of the RVE bi-soliton. (a),(b) Surface profiles $\eta(x)$ at minimum and maximum amplitude, respectively. (c) Stable trajectories of soliton eigenvalues with $T \approx 30.0$. Blue and red lines correspond to two complete cycles of the bi-soliton oscillations separated by 200 T.

presented in Supplemental Material [44]. Note that in the case of the RVE bi-solitons, the IST perturbation theory works only quantitatively, which is expected for the fully nonlinear model due to the presence of the complicated structure of its rhs.

The IST analysis of the long-living bi-solitons in the deep water models shows that these oscillatory complexes exist in a stable nearly integrable regime and can be described within the IST perturbation theory. In general, the governing DZE and RVE models are far from being integrable; however, for the bi-solitons all the rhs terms are small throughout the whole oscillation period T. The numerically computed time series of the IST spectrum allows us to accurately reveal the recursive dynamics of the bi-solitons preserving at the scale of hundreds of T. We also show that the bi-soliton complex is stabilized by minor radiation and a nonzero velocity difference between solitons; both of them gradually increase up to the high-amplitude wave field configuration so that the two discrete components and continuous part of the scattering data are in periodic energy and momentum exchange.

In contrast to the approximately solvable models with weakly interacting solitons [65–70], the bi-solitons considered here are fully overlapping and governed by equations of type (7) with such complicated rhs's that cannot be studied analytically with the perturbation framework (12). Here, we propose a perspective of using IST theory in such nonsolvable cases based on the combination of the perturbation approach, exact multisoliton solutions, and numerical IST tools. Our approach provides an IST interpretation of the interaction mechanism for the deep water bi-solitons and opens questions for further studies. One of them is identifying a complete set of initial soliton eigenvalues corresponding to long-living recursive bi-soliton dynamics. Another question concerns the connection of the presented approach with general methods of finding periodic solutions to nonlinear PDEs [71,72]. Besides localized solitonic wave fields, considering a continuous wave background is of fundamental interest for the comparative study of the deep fluid models in the light of the proposed IST approach [32,73,74]. In particular, a combination of the IST with Melnikov's analysis being applied to the DZE and RVE can shed new light on behavior of the so-called breathers—solitons living on the background [75–78]. Our results can be generalized to other physical systems, such as optical waveguides described in the leading order by the NLSE [4,56], and also applied to analyze experimental data.

The work of A. G. was funded by the European Union's Horizon 2020 research and innovation program under the Marie Skłodowska-Curie Grant Agreement No. 101033047. The work of S. D. and D. K. on obtaining and studying bi-solitons in the deep fluid models was supported by the RSF Grant No. 19-72-30028-II. The work of R. M. on IST perturbation theory analysis was supported by RSF Grant No. 19-79-30075-II.

*Corresponding author: Andrey.Gelash@u-bourgogne.fr
Present address: Institute of Physics, Swiss Federal Institute of Technology Lausanne (EPFL), CH-1015 Lausanne, Switzerland.

[1] V. E. Zakharov and E. A. Kuznetsov, Phys. Usp. **55**, 535 (2012).
[2] M. Remoissenet, *Waves Called Solitons: Concepts and Experiments* (Springer Berlin Heidelberg, Berlin, Germany, 2013).
[3] A. Ankiewicz and N. Akhmediev, *Dissipative Solitons: From Optics to Biology and Medicine* (Springer, New York, 2008).
[4] Y. S. Kivshar and G. Agrawal, *Optical Solitons: From Fibers to Photonic Crystals* (Academic Press, Amsterdam, 2003).
[5] J. M. Soto-Crespo, M. Grapinet, P. Grelu, and N. Akhmediev, Phys. Rev. E **70**, 066612 (2004).
[6] U. Al Khawaja and H. Stoof, New J. Phys. **13**, 085003 (2011).
[7] M. Stratmann, T. Pagel, and F. Mitschke, Phys. Rev. Lett. **95**, 143902 (2005).
[8] P. Grelu and N. Akhmediev, Nat. Photonics **6**, 84 (2012).
[9] S. Novikov, S. Manakov, L. Pitaevskii, and V. Zakharov, *Theory of Solitons: The Inverse Scattering Method* (Springer Science & Business Media, New York City, 1984).
[10] Y. S. Kivshar and B. A. Malomed, Rev. Mod. Phys. **61**, 763 (1989).
[11] L. D. Faddeev and L. A. Takhtajan, *Hamiltonian Methods in the Theory of Solitons* (Springer Science & Business Media, Berlin, 2007).
[12] G. Berman and F. Izrailev, Chaos **15**, 015104 (2005).
[13] M. J. Ablowitz and H. Segur, *Solitons and the Inverse Scattering Transform* (SIAM, Philadelphia, 1981), Vol. 4.
[14] V. E. Zakharov and A. B. Shabat, Sov. Phys. JETP **34**, 62 (1972), http://www.jetp.ras.ru/cgi-bin/dn/e_034_01_0062.pdf.

[15] A. V. Buryak and N. N. Akhmediev, Phys. Rev. E **50**, 3126 (1994).
[16] J. A. Besley, P. D. Miller, and N. N. Akhmediev, Phys. Rev. E **61**, 7121 (2000).
[17] V. E. Zakharov, J. Appl. Mech. Tech. Phys. **9**, 190 (1968).
[18] A. Dyachenko, D. Kachulin, and V. E. Zakharov, J. Ocean Eng. Marine Energy **3**, 409 (2017).
[19] L. V. Ovsyannikov, Sib. Branch Acad. Sci. USSR **15**, 104 (1973).
[20] S. Tanveer, Proc. R. Soc. A **435**, 137 (1991).
[21] A. Dyachenko, E. Kuznetsov, M. Spector, and V. Zakharov, Phys. Lett. A **221**, 73 (1996).
[22] A. I. Dyachenko, in *Doklady Mathematics* (Pleiades Publishing, Ltd., Road Town, UK, 2001), Vol. 63, pp. 115–117.
[23] A. Dyachenko, D. Kachulin, and V. Zakharov, J. Fluid Mech. **828**, 661 (2017).
[24] A. V. Slunyaev and V. I. Shrira, J. Fluid Mech. **735**, 203 (2013).
[25] M. Onorato, D. Proment, G. Clauss, and M. Klein, PLoS One **8**, e54629 (2013).
[26] A. Tikan, F. Bonnefoy, G. Roberti, G. El, A. Tovbis, G. Ducrozet, A. Cazaubiel, G. Prabhudesai, G. Michel, F. Copie *et al.*, Phys. Rev. Fluids **7**, 054401 (2022).
[27] A. I. Dyachenko and V. E. Zakharov, JETP Lett. **88**, 307 (2008).
[28] A. Slunyaev, J. Exp. Theor. Phys. **109**, 676 (2009).
[29] A. Slunyaev, G. F. Clauss, M. Klein, and M. Onorato, Phys. Fluids **25**, 067105 (2013).
[30] A. Slunyaev, M. Klein, and G. F. Clauss, Phys. Fluids **29**, 047103 (2017).
[31] F. Fedele and D. Dutykh, J. Fluid Mech. **712**, 646 (2012).
[32] D. Kachulin, A. Dyachenko, and V. Zakharov, Fluids **5**, 67 (2020).
[33] D. Kachulin, A. Dyachenko, and S. Dremov, Fluids **5**, 65 (2020).
[34] D. Kachulin, S. Dremov, and A. Dyachenko, Fluids **6**, 115 (2021).
[35] H. Lamb, *Hydrodynamics* (University Press, Cambridge, UK, 1924).
[36] V. E. Zakharov, V. S. L'vov, and G. Falkovich, *Kolmogorov Spectra of Turbulence 1. Wave Turbulence* (Springer-Verlag, Berlin (Germany), 1992).
[37] C. Kharif, E. Pelinovsky, and A. Slunyaev, *Rogue Waves in the Ocean, Observation, Theories and Modeling*, Advances in Geophysical and Environmental Mechanics and Mathematics Series (Springer, Heidelberg, 2009).
[38] A. Osborne, *Nonlinear Ocean Waves* (Academic Press, New York, 2010).
[39] G. Ducrozet, F. Bonnefoy, D. Le Touzé, and P. Ferrant, Comput. Phys. Commun. **203**, 245 (2016).
[40] F. Fedele, J. Fluid Mech. **748**, 692 (2014).
[41] A. Dyachenko, S. Dyachenko, P. Lushnikov, and V. Zakharov, Proc. R. Soc. A **477**, 20200811 (2021).
[42] A. Dyachenko, S. Dyachenko, and V. Zakharov, J. Fluid Mech. **952**, A30 (2022).
[43] R. Stuhlmeier and M. Stiassnie, J. Fluid Mech. **913**, A50 (2021).
[44] See Supplemental Material at http://link.aps.org/supplemental/10.1103/PhysRevLett.132.133403 for details, which includes Ref. [45].
[45] A. Korotkevich, A. Pushkarev, D. Resio, and V. E. Zakharov, Eur. J. Mech. B **27**, 361 (2008).
[46] S. Randoux, P. Suret, A. Chabchoub, B. Kibler, and G. El, Phys. Rev. E **98**, 022219 (2018).
[47] I. S. Chekhovskoy, O. Shtyrina, M. P. Fedoruk, S. B. Medvedev, and S. K. Turitsyn, Phys. Rev. Lett. **122**, 153901 (2019).
[48] P. Suret, A. Tikan, F. Bonnefoy, F. Copie, G. Ducrozet, A. Gelash, G. Prabhudesai, G. Michel, A. Cazaubiel, E. Falcon *et al.*, Phys. Rev. Lett. **125**, 264101 (2020).
[49] S. K. Turitsyn, I. S. Chekhovskoy, and M. P. Fedoruk, Opt. Lett. **45**, 3059 (2020).
[50] A. Slunyaev, Phys. Fluids **33** (2021).
[51] I. Teutsch, M. Brühl, R. Weisse, and S. Wahls, Natural Hazards and Earth System Sciences **23**, 2053 (2022), 10.5194/nhess-23-2053-2023.
[52] D. S. Agafontsev, A. A. Gelash, R. I. Mullyadzhanov, and V. E. Zakharov, Chaos Solitons Fractals **166**, 112951 (2023).
[53] V. B. Matveev and M. A. Salle, *Darboux Transformations and Solitons* (Springer-Verlag, Berlin, 1991).
[54] D. J. Kaup, SIAM J. Appl. Math. **31**, 121 (1976).
[55] V. I. Karpman and E. M. Maslov, Sov. Phys. JETP **46**, 281 (1977), http://www.jetp.ras.ru/cgi-bin/dn/e_046_02_0281.pdf.
[56] J. Yang, *Nonlinear Waves in Integrable and Nonintegrable Systems* (SIAM, Philadelphia, USA, 2010), Vol. 16.
[57] F. Coppini, P. G. Grinevich, and P. M. Santini, Phys. Rev. E **101**, 032204 (2020).
[58] R. Mullyadzhanov and A. Gelash, Phys. Rev. Lett. **126**, 234101 (2021).
[59] G. Boffetta and A. R. Osborne, J. Comput. Phys. **102**, 252 (1992).
[60] R. Mullyadzhanov and A. Gelash, Opt. Lett. **44**, 5298 (2019).
[61] A. Gelash and R. Mullyadzhanov, Phys. Rev. E **101**, 052206 (2020).
[62] J. P. Boyd, *Weakly Nonlocal Solitary Waves and Beyond-All-Orders Asymptotics: Generalized Solitons and Hyper-asymptotic Perturbation Theory* (Springer Science & Business Media, 2012), Vol. 442.
[63] J. Yang, B. A. Malomed, and D. J. Kaup, Phys. Rev. Lett. **83**, 1958 (1999).
[64] K. Khusnutdinova, Y. Stepanyants, and M. Tranter, Phys. Fluids **30** (2018).
[65] V. Karpman and V. Solov'ev, Physica D (Amsterdam) **3D**, 487 (1981).
[66] K. Gorshkov and L. Ostrovsky, Physica (Amsterdam) **3D**, 428 (1981).
[67] K. Gorshkov, L. Ostrovsky, V. Papko, and A. Pikovsky, Phys. Lett. **74A**, 177 (1979).
[68] V. S. Gerdjikov, D. J. Kaup, I. M. Uzunov, and E. G. Evstatiev, Phys. Rev. Lett. **77**, 3943 (1996).
[69] J. Yang, Phys. Rev. E **64**, 026607 (2001).
[70] Y. Zhu and J. Yang, Phys. Rev. E **75**, 036605 (2007).
[71] D. M. Ambrose and J. Wilkening, J. Nonlinear Sci. **20**, 277 (2010).

[72] J. Wilkening and J. Yu, Comput. Sci. Discovery **5**, 014017 (2012).
[73] V. E. Zakharov and L. Ostrovsky, Physica (Amsterdam) **238D**, 540 (2009).
[74] A. Gelash, D. Agafontsev, V. Zakharov, G. El, S. Randoux, and P. Suret, Phys. Rev. Lett. **123**, 234102 (2019).
[75] C. Schober, Eur. J. Mech.-B/Fluids **25**, 602 (2006).
[76] C. M. Schober, in *Dynamics and Bifurcation of Patterns in Dissipative Systems* (World Scientific, Singapore, 2004), pp. 194–213.
[77] N. N. Akhmediev and A. Ankiewicz, *Nonlinear Pulses and Beams* (Springer, New York, 1997).
[78] I. Mullyadzhanov, A. Gudko, R. Mullyadzhanov, and A. Gelash, Proc. R. Soc. A **480**, 20230529 (2024).